Available online at www.sciencedirect.com
SCIENCE DIRECT
Journal of Nuclear Materials 347 (2005) 1–11
journal of nuclear materials
www.elsevier.com/locate/jnucmat

Immobilization of fission products arising from pyrometallurgical reprocessing in chloride media

G. Leturcq *, A. Grandjean, D. Rigaud, P. Perouty, M. Charlot

CEA Marcoule DTCD, BP 17171, 30207 Bagnols sur Cèze, France

Received 4 January 2005; accepted 14 June 2005

Abstract

Spent nuclear fuel reprocessing to recover energy-producing elements such as uranium or plutonium can be performed by a pyrochemical process. In such method, the actinides and fission products are extracted by electrodeposition in a molten chloride medium. These processes generate chlorinated alkali salt flows contaminated by fission products, mainly Cs, Ba, Sr and rare earth elements constituting high-level waste. Two possible alternatives are investigated for managing this wasteform; a protocol is described for dechlorinating the fission products to allow vitrification, and mineral phases capable of immobilizing chlorides are listed to allow specification of a dedicated ceramic matrix suitable for containment of these chlorinated waste streams. The results of tests to synthesize chlorosilicate phases are also discussed.

1. Introduction

In order to recover high-energy elements such as uranium or plutonium, the reprocessing of spent nuclear fuel can be performed by a pyrochemical process [1]. In one such method developed at the Argonne National Laboratory [2], the actinides and fission products are extracted by electrodeposition in a molten chloride medium. This extraction process is based on the distribution of the elements between a dense liquid or solid phase in which the elements are present in the metallic state, and a salt phase in which the elements are present as chlorides. Reprocessing then comprises several successive steps: separation of the reducible elements (noble metals and other elements: Mo, Pd, Tc, Ru, Rh, Zr), separation of the actinides and lanthanides, and treatment of the bath for recycling.

During extraction, the chloride bath becomes concentrated with radionuclide chlorides including alkali metals (Cs, Na, etc.), alkaline earth metals (Sr, Ba) and a few rare earth elements. These fission products significantly modify the physical and chemical characteristics of the salt, e.g. by increasing the salt melting point and contaminating the extraction cathode with fission products. The chlorinated salt must then be regenerated or replaced. Since it contains radionucleides such as ^{137}Cs and ^{90}Sr the salt is a high-level waste and highly water-soluble thus requires a specific treatment to insure

* Corresponding author. Tel.: +33 4 66 79 63 76; fax: +33 4 66 79 18 80.
E-mail address: gilles.leturcq@cea.fr (G. Leturcq).

0022-3115/$ - see front matter © 2005 Elsevier B.V. All rights reserved.
doi:10.1016/j.jnucmat.2005.06.026

the final immobilization of these radionucleides. It is impossible to include chlorides into a silicate glass at acceptable concentrations. However due to a too high chloride concentration this waste stream therefore cannot be vitrified as is [3,4].

Two alternatives are possible for managing this high-level wasteform:

- Specifically process the salt to convert the chlorides to oxides suitable for conventional immobilization of the FP by vitrification.
- Develop a specific ceramic matrix for this wasteform. The work described in the literature on this subject – particularly at the Argonne National Laboratory – led to the selection of a glass-bonded sodalite composite matrix comprising a sodalite phase $(Na,K)_8Al_6Si_6O_24Cl_2$ incorporating the alkalis and chlorine, embedded in a vitreous phase to accommodate the other fission products, i.e. mainly alkaline earth and rare earth elements [5,6]. The chemical durability of such matrix was tested and found to be in the order of 0.05 g m^{-2} d^{-1} [7].

Both alternatives were considered in this study. A fission product dechlorination protocol is proposed, and mineral phases capable of immobilizing chlorides are listed. The results of tests dedicated to the preparation of chlorosilicate phases are also discussed.

2. Results

2.1. Dechlorination of FP-contaminated salts for conventional immobilization in an oxide glass

The objective was to develop a specific treatment for the chlorinated salt generated by pyrochemical reprocessing of spent fuel in a chlorinated medium, in order to convert the chloride cations to oxides and recover the chlorine in a form compatible with immobilization in a suitable ceramic matrix. The oxidized cations could be easily loaded in a borosilicate glass in a conventional melting process.

We propose the following flowsheet (Fig. 1):

1. Solubilization of all the chlorides in ultrapure water.
2. Precipitation of the dissolved rare earth elements (Ce^{3+}, Nd^{3+}, La^{3+}, Y^{3+}) and alkaline earth metals (Ba^{2+}, Sr^{2+}) as oxides by adding of potassium hydroxide (KOH) and filtration.
3. Precipitation of the dissolved Cl^- by silver oxide (Ag_2O) to form insoluble silver chloride (AgCl) and filtration. Note that the AgCl product solubility in water at 25 °C is equal to $10^{-9.7}$.
4. The rare earth and alkaline earth oxides plus the aqueous solution containing only a minimum amount of dissolved chlorine are now suitable for containment in an appropriate borosilicate glass.

The recovered silver chloride can be submitted to a specific reprocessing to recover silver as Ag_2O for recycling in step 3. Chlorine would then be immobilized in a specific matrix. Silver chloride could also be melted to form pellets ($T_f = 454.85$ °C). Then, provided it meets the immobilization criteria, especially durability, it could be used as a chlorine containment matrix.

From a thermodynamic point of view [8], it should be possible to treat AgCl with hydrogen at 300 °C to form metallic silver that could be oxidized for recycling in step 3. Hydrogen chloride could then be used to synthesize a salt suitable for the pyrometallurgical separation process (to be tested).

The conversion process steps were tested at laboratory scale. The test salt composition (Table 1) was taken from the literature [6]. For greater simplicity, $NdCl_3$, $LaCl_3$ and YCl_3 were replaced by $CeCl_3$, and $SrCl_2$ was replaced by $BaCl_2$.

Dissolving 10 g of salt in 500 mL of water and adding 0.49 g of KOH (corresponding to 5 moles of KOH for 100 moles of chlorides) resulted in the production of 1.23 g of a yellow hydrated precipitate; 19.14 g of Ag_2O were then added to the aqueous solution, corresponding to a slightly superstoichiometric (about 0.9%) quantity of Ag to allow the quantitative precipitation of Cl^-. An AgCl precipitate was obtained, as confirmed by SEM/EDS analysis of the powder obtained after drying. The filtrate was diluted, then ICP/MS analysis for cations and ion chromatography analysis for Cl^- yielded the results indicated in Table 2.

- The resulting low Cl concentration (1.2×10^{-3} M) could be minimized by increasing the Ag_2O feeding. However, it will not be possible to remove all the dissolved chlorine as its concentration is also controlled by AgCl solubility ($pKs = 9.7$ at 25 °C).
- Small quantities of Ba (1.6×10^{-4} M) also remained in solution, indicating incomplete precipitation of $Ba(OH)_2$. This could be improved

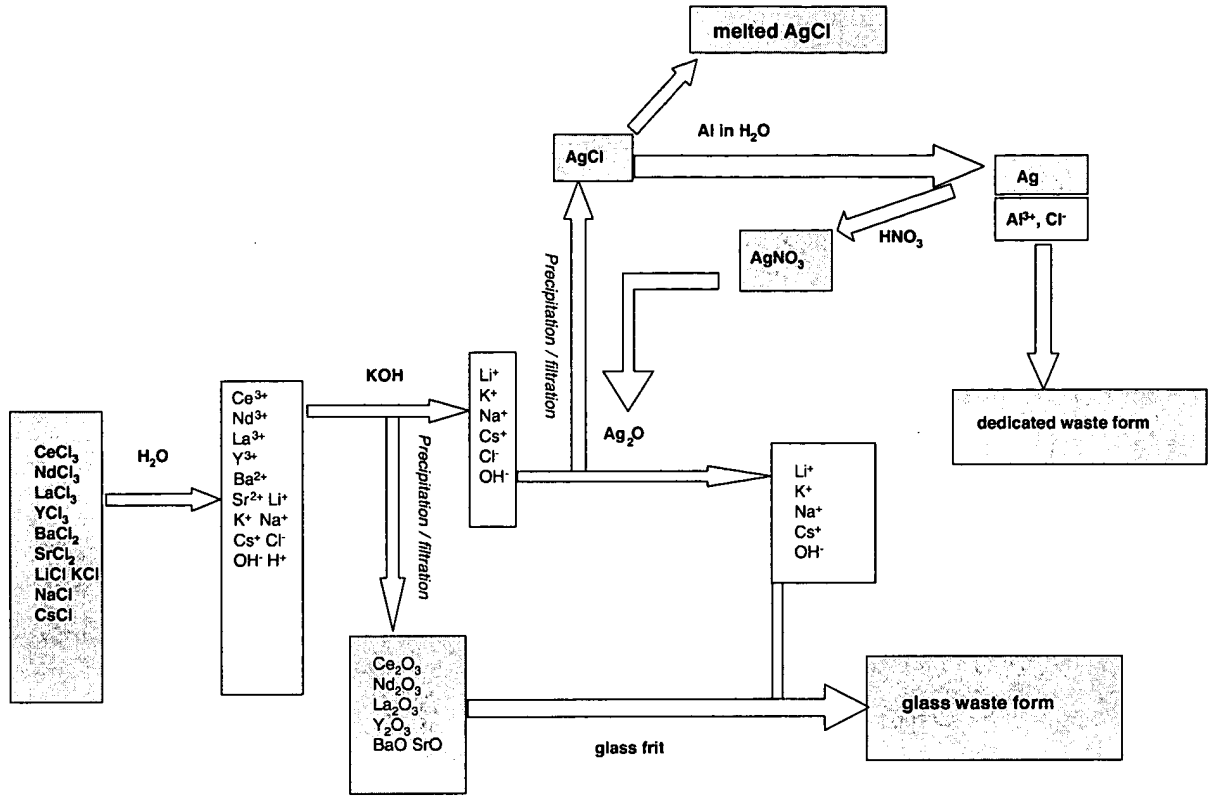

Fig. 1. Flowsheet for conversion of contaminated chlorinated salt into oxides with EDS spectra identifying the nature of the silver precipitates and SEM image of AgCl pellet sintered at 300 °C for 10 h in air.

Table 1
Composition of chlorides (mol%)

Salt	Mol%
$CeCl_3$	0.73
$BaCl_2$	0.63
CsCl	1.32
LiCl	55.15
KCl	35.96
NaCl	6.10

Table 2
Composition of filtrate obtained after separation of AgCl precipitate obtained by adding Ag_2O

Element	M
Ce	$<7 \times 10^{-6}$
Ba	1.6×10^{-4}
Cs	8.1×10^{-4}
Li	2.7×10^{-2}
K	3.9×10^{-2}
Na	3.3×10^{-3}
Ag	1.5×10^{-6}
Cl	1.2×10^{-3}

by pH adjustment. However, the Ba leftover stayed in solution after the addition of silver oxide due to a high dilution and therefore it was separated from chloride ions as alkaline metals.

- Only a minimal fraction of the Ag entered solution (1.5×10^{-6} M).

2.2. Immobilization of cations remaining in solution from the first precipitate

Based on the analyzed cation composition and the Cl^- concentration, the oxide mass concentration of the waste stream was calculated to assess whether this waste could be immobilized in a conventional borosilicate glass; the first precipitate containing all the initial cerium and a fraction of the barium was considered.

The preliminary results (Table 3) suggest that by designing suitable formulations it should be possible to immobilize this waste stream with about 20 wt% of this waste loading in a borosilicate glass [9].

Table 3
Composition of oxides and chlorine in the waste vitrification feed stream (wt%)

Oxide	Wt%
Ln_2O_3	7.09
BaO	5.71
Cs_2O	4.00
Li_2O	14.18
K_2O	64.00
Na_2O	3.53
Cl	1.47
Ag_2O	0.01

Disposition of the AgCl precipitate: Two routes are possible for the recovered AgCl precipitate:

1. The first one is to consider AgCl as a containment material for chlorine and any remaining impurities in the precipitate. Melting at 500 °C was attempted with success and without any mass lost, leading to a full density chlorargyrite. The physical and chemical characteristics of this material (durability, mechanical strength, microstructure, homogeneity, etc.) must be further investigated.
2. The second one would be to recover the silver contained in the AgCl, reoxidize this Ag and recycle it as Ag_2O during the chloride precipitation step. This route involves a larger number of steps, but has an appreciable advantage in that it does not consume Ag in the complete cycle.

AgCl reduction by aluminum chips was tested in aqueous media. The theoretical equation is the following:

$$3AgCl + Al \rightarrow 3Ag + Al^{3+} + 3Cl^-$$

This reaction is in competition with $Al + 3H_2O \rightarrow 3H_2 + Al_2O_3$.

The AgCl precipitate obtained during the preceding step was mixed with a large quantity of metallic aluminum chips. The AgCl was converted to Ag metal, forming a pile with the metallic aluminum and creating a side reaction releasing dihydrogen (bubbles were observed to form); a fraction of the aluminum was converted to alumina, inhibiting the previous reaction. The precipitate was then filtered and observed by SEM/EDS. The results revealed the presence of remaining silver chloride. Nevertheless, this is a promising route requiring further investigation. Indeed, as instance, the use of Al powder and/or another solvent could increase the reaction yield.

2.3. Immobilization of $AlCl_3$ from the FP-contaminated salt dechlorination cycle

2.3.1. Wadalite synthesis

Wadalite ($Ca_6Al_5Si_2O_{16}Cl_3$) was the first material investigated because of its potential use for immobilizing aluminum chloride, which could be produced in the process of converting the chlorinated stream to oxyhydroxides (Fig. 2). A mixture of 21.19 g of CaO, 15.21 g of $AlCl_3(6H_2O)$, 12.84 g of Al_2O_3, and 7.57 g of SiO_2 was heated to 800 °C for 2 h. The XRD diagram of the resulting powder is shown in Fig. 2.

The reaction was apparently incomplete, and several phases were observed:

- wadalite, as expected,
- some residual quartz (SiO_2) and corundum (Al_2O_3),
- apparently a second phase containing chlorine but no aluminum ($Ca_3SiO_4Cl_2$).

A pressure-assisted sintering test of this powder was carried out after firing at 800 °C. The powder was pressed for 2 h at 100 MPa in a die heated to 250 °C. The pellet density estimated by dimensional measurement was 2.1 (i.e. 70% of the calculated density). The pellet was examined by SEM/EDS (Fig. 3), confirming that the sample was porous and included two chlorinated phases, one of which was light-colored and contained no aluminum.

Thermogravimetric analysis of the powder (Fig. 4) revealed:

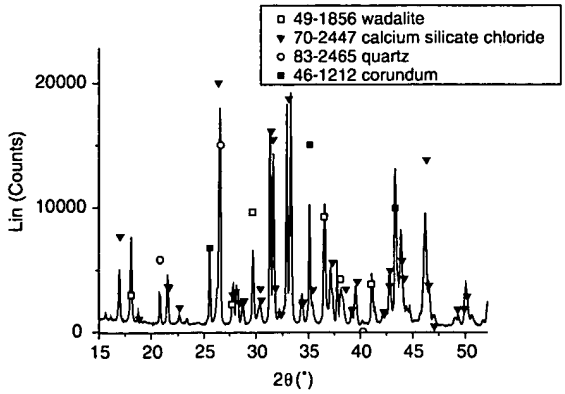

Fig. 2. XRD diagram of powder batch containing SiO_2, CaO, Al_2O_3, $AlCl_3$ in stoichiometric proportions for wadalite, heat-treated for 2 h at 800 °C.

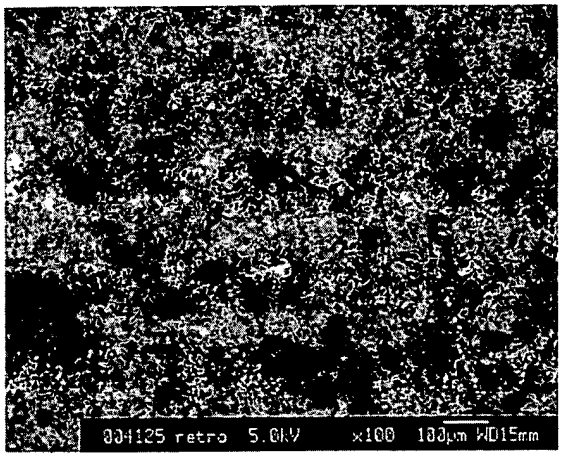

Fig. 3. (a) SEM image and (b) X-EDS analysis of wadalite pellet sintered at 250 °C and 100 MPa for 2 h.

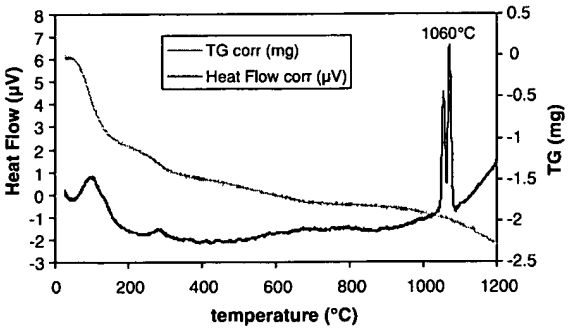

Fig. 4. DTA/TGA of wadalite powder after heating for 2 h at 800 °C.

- about 1% mass loss up to 400 °C,
- two exothermic peaks near 1060 °C (tone could correspond to the larnite crystallization),
- no significant mass loss up to 1200 °C.

These encouraging results led us to test a heat treatment at 1100 °C to enhance the formation of wadalite formation reaction. Two heating times were tested: 1 h and 10 h. Both powder were characterized by XRD. Even after 10 h of heat treatment the reaction was incomplete (system composed of wadalite, calcium chlorosilicate and corundum) although wadalite became the major phase as the larnite disappeared and the intensity of the corundum and calcium chlorosilicate phases decreased in the XRD diagram (Fig. 5).

Microstructural observation of the powder treated for 10 h (Fig. 6) showed that the resulting crystals measured about 20 µm, with a platty form poorly suited for sintering: a natural sintering test with a pellet pressed at 120 MPa from this powder for 5 h at 1100 °C resulted in only 75% of densification ($d = 2.3$).

Another test of wadalite synthesis by the alkoxide route was also performed. A mixture of tetraethoxysilane and aluminum sec-butoxide diluted in ethanol was added to a solution of calcium nitrate

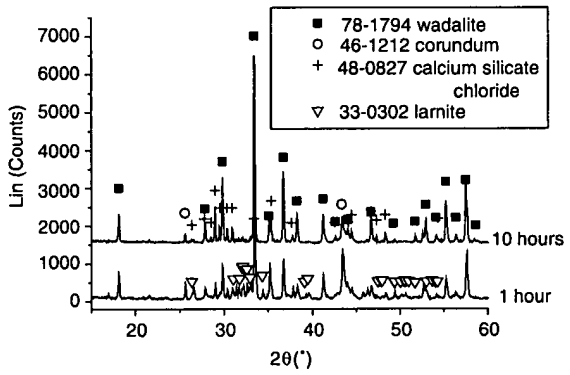

Fig. 5. XRD diagram of powder batch containing SiO_2, CaO, Al_2O_3, $AlCl_3$ in stoichiometric proportions for wadalite, heat-treated for 1 and 10 h at 1100 °C.

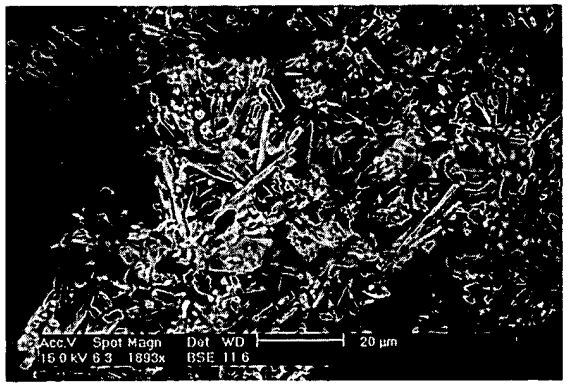

Fig. 6. SEM image of wadalite powder after firing for 10 h at 1100 °C.

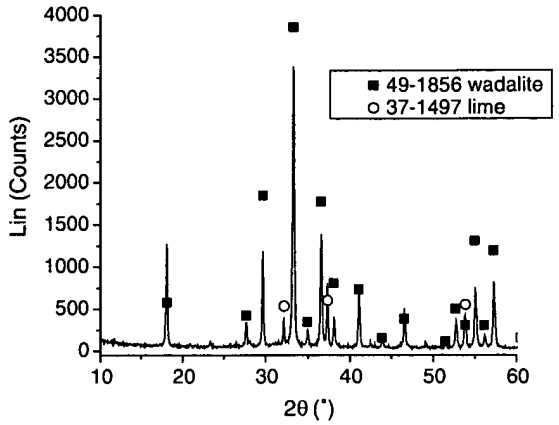

Fig. 7. XRD diagram of wadalite powder obtained by the alkoxide route and heat-treated for 2 h at 800 °C.

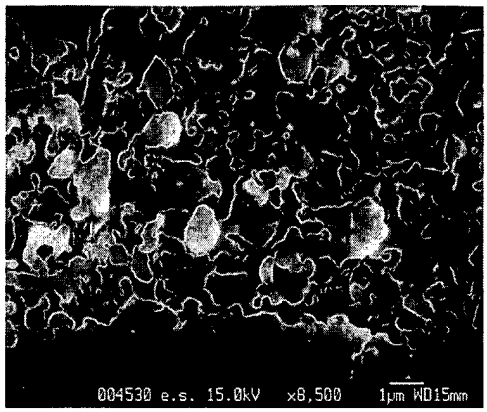

Fig. 8. Scanning electron microscope image of $Ca_3SiO_4Cl_2$ pellet sintered at 700 °C.

and aluminum chloride dissolved in ultrapure water. After evaporation of the solvent then drying at 120 °C, the precipitate was heated for 2 h at 800 °C. The powder was then characterized by XRD (Fig. 7), revealing mainly wadalite together with the minor phase, CaO (lime). Due to its high hygroscopic behavior, the formation of such minor phase has to be prevented especially because it will lead to high pH value when the sample is leached in water, enhancing the corrosion of the material.

2.3.2. Calcium chlorosilicate

As the chlorine weight amount of $Ca_3SiO_4Cl_2$ is twice the wadalite chlorine contain, potentially there is an interest to immobilize chlorine in such waste-form. By adding CaO to $AlCl_3$ and heating this mixture up to 200 °C, $CaCl_2$ and aluminum oxide are formed. By dissolving $CaCl_2$, it is then possible to separate this phase from aluminum oxide by filtration. Then it is possible to confine the $CaCl_2$, coming from this evaporated solution, in $Ca_3SiO_4Cl_2$ wasteform. Indeed this phase can be synthesized by heating at 700 °C for 3 h a mixture of $CaCl_2$, CaO and SiO_2 in stoichiometric proportion. The XRD analysis of the obtained powder revealed that $Ca_3SiO_4Cl_2$ is the major phase with another calcium chlorosilicate depleted in calcium chloride. Natural sintering was carried out at 700 °C on a 75 MPa uniaxial-pressed pellet and led to a porous but homogeneous sample as shown in Fig. 8.

These findings support not only the feasibility to convert the fission-product-bearing chlorinated salt stream into oxides suitable for vitrification, but also to immobilize chlorine in various forms – particularly chlorargyrite, wadalite or calcium chlorosilicate – although this aspect requires optimized.

2.3.3. Immobilization of chlorinated salts contaminated with fission products in a dedicated matrix

In order to address the second research issue concerning chlorinated effluent management, we investigated crystalline phases capable to load chlorides. Our approach was to identify natural mineral phases with appreciable chlorine concentrations, in addition to synthetic crystalline phases listed in the JCPDS files (Table 4). Several chemical families are capable to immobilize chlorides: including chlorosilicates, chlorovanadates, chlorotungstates, chlorochromates, chloroselenates, and chloroniobiates. Within each chemical family, the phases are classified by decreasing chlorine weight content. Density and hardness values are provided when available, as they are indicative of the potential suitability of the crystalline phase for containment (a containment matrix must be mechanically stable, and the density and waste loading can be used to estimate the resulting waste package volume). No attempt has yet been made to obtain leaching resistance data. The mineral group is also indicated for the natural phases to provide further information on their crystal structure. Finally, as the objective is to immobilize simultaneously chlorine and fission product chlorides, the chemical composition of each phase – and especially the number of cationic sites – must be considered in assessing its suitability for immobilization of alkalis, alkaline earths and rare earth elements. Crystalline or compatible glass–ceramic composites can also

Table 4
Crystalline phases containing chlorine

Chemical composition	Name	Mineral group	Density	Mohs hardness	Cl (wt%)
Silicates					
$Ca_3SiO_4Cl_2$					25.0
$Ca_6Al_5Si_2O_{16}Cl_3$	Wadalite	Feldspathoid/sodalite	3.06		12.9
$(Na,K)_6Ca_2Al_6Si_6O_{24}Cl_2$	Quadridavyne	Feldsathoid/cancrinite	2.335	5	12.2
$Na_3K_6Ti_2Al_2Si_8O_{26}Cl_3$	Altisite	Phyllosilicate	2.65	6	8.9
$Na_4AlBeSi_4O_{12}Cl$	Tugtupite	Feldspathoid/sodalite	2.36	4	7.6
$Na_8Si_6Al_6O_{24}Cl_2$	Sodalite	Feldspathoid/sodalite	2.29	6	7.3
$NaCa_2Fe_4AlSi_6Al_2O_{22}Cl_2$	Ferrochloropargasite	Amphibole	~3	5–6	7.1
Vanadates					
$Ln_3VO_4Cl_6$					28
Ca_2VO_4Cl					15.4
$PbCu_3VO_4Cl_2$	Leningradite	Carminite	4.8	4.5	12.2
KBa_2V_2O7Cl					6.3
$Pb_{14}(VO_4)_2O_9Cl_4$	Kombatite				4.2
$Pb_5(VO4)_3Cl$	Vanadinite	Apatite	6.9	3.5–4	2.5
Selenates					
$KCdCu_7O_{12}Se_4O_6Cl_9$	Burnsite			1–1.5	25
$Zn_2SeO_3Cl_2$	Sophiite			2–2.5	21.6
$Cu_9O_2(SeO_3)_4Cl_6$	Chloromenite			1.5–2.5	16
$NaCu_5O_2(SeO_3)_2Cl$	Ilinskite		4.08	1.5–2	5.4
$Cu_3Bi(SeO_3)_2O_2Cl$	Francisite			3–4	4.9
Tungstates					
A_2WOCl_5					27.6–45.3
$A_2WO_2Cl_4$					22.7–38.2
AWO_2Cl_2					16.9–24.1
$Ca_3WO_5Cl_2$					15.6
$Ln_3WO_6Cl_3$					13
$FeWO_4Cl$					10.5
$LnWO_4Cl$					8.3
$Pb_3WO_5Cl_2$	Pinalite				7.4
Chromates					
Cs_2CrOCl_5					34.8
$ACrO3Cl$					13.3–24.9
Ca_2CrO_4Cl					15.3
Sr_2CrO_4Cl					10.9
$Ca_5(CrO_4)_3Cl$					6.1
$Sr_5(CrO_4)_3Cl$					4.3
$Ba_{8.5}Cr_5AlO_{24}Cl_2$					3.7
$Pb_{10}(CrO_4)_3(SiO_4)_3Cl_2$	Bellite				2.6
Niobiates					
$Pr_3NbO_4Cl_6$					26.8
Nb_3O_7Cl					8.3
$LaNb_2O_6Cl$					7.8
Other					
$La_2TaO_4Cl_3$					16.9
$Nd_2Ta_2O_7Cl_2$					8.5
$FeMn_7O_{10}Cl_3$					15
$Sr_3Ga_2O_5Cl_2$					12.8
$Pb_6As_2O_7Cl_4$	Eliophyllite				8.6
$Pb_3MoO_5Cl_2$					8.2
$Ca_5(PO_4)_3Cl$	Chloroapatite				6.8

A: alkalis; Ln: lanthanides.

be considered for immobilizing chlorinated fission products.

Selenates compounds exhibit low hardness, and can be ruled out at the outset, as can the niobates

for reasons of cost. This leaves four promising chemical families: chlorosilicates, chlorovanadates, chlorochromates and chlorotungstates.

Following the inventory of chlorinated phases we began testing chlorosilicate synthesis processes.

Sodalite($Na_8Al_6Si_6O_{24}Cl_2$) matrices: The Argonne National Laboratory has developed a composite glass-bonded sodalite ceramic to immobilize chlorinated fission products arising from a pyrochemical process [6]. In this process, chlorinated fission products are confined in zeolite, which is then mixed with glass frit and hot-pressed to form a glass-bonded sodalite composite. The vitreous phase ensures satisfactory sintering and makes it unnecessary to load all the fission products in the sodalite structure. The drawback of this process is its complexity (use of a high-temperature isostatic press). Other sodalite synthesis routes have been developed. The 'thermal' method described by Koyama et al. [10,11] consists in a heat treatment of a mixture of sodium hydroxide, alumina and silica between 250 and 600 °C for 2–20 h in dry atmosphere to form an anhydrous intermediate reaction product comprising $NaAlO_2$, Na_2SiO_3 and Al_2O_3. The anhydrous powder is then added to the salt and hot pressed between 250 °C and 500 °C at pressures ranging from 10 to 70 MPa for 1–8 h to obtain a compact pellet. The pellet is subsequently heated between 700 °C and 900 °C for 20–200 h to prepare sodalite. Hydrothermal synthesis routes have also been successfully evaluated in many cases, but requiring more difficult techniques and longer synthesis times: for synthesizing a 'nitric' sodalite $Na_8(AlSiO_4)(NO_2)_{2-x}(NO_3)_x$ [12,13], a 'hydrosodalite' $Na_8(SiAlO_4)_6(OH)_2$ [14], and a 'chlorinated' sodalite [15].

We first considered the synthesis of sodalite from an uncontaminated salt consisting of 0.4 mole KCl and 0.6 mole LiCl. Like Koyama, we found it necessary to use an anhydrous intermediate reaction product, as the reaction between the salt and a mixture of sodium hydroxide, alumina, silica and sodium chloride did not yield to sodalite. We chose nepheline ($NaAlSiO_4$) as the intermediate reaction product, however, rather than an anhydrous powder mixture as suggested by Koyama et al. [10,11]. Nepheline was synthesized from kaolinite ($Al_2Si_2O_7$, $2H_2O$) and sodium hydroxide (NaOH) by heating at 700 °C for 2 h. The material was characterized by XRD and revealed the nepheline crystallization. The second step was to initiate a reaction between nepheline, potassium chloride and lithium chloride in stoichiometric conditions ($Na_6K_{0.8}Li_{1.2}Al_6Si_6O_{24}Cl_2$) for 48 h at 700 °C.

Following this reaction the powder consisted exclusively of sodalite (as shown in Fig. 9). Thermogravimetric analysis showed mass loss above 830 °C, apparently reaching a peak at 1070 °C as

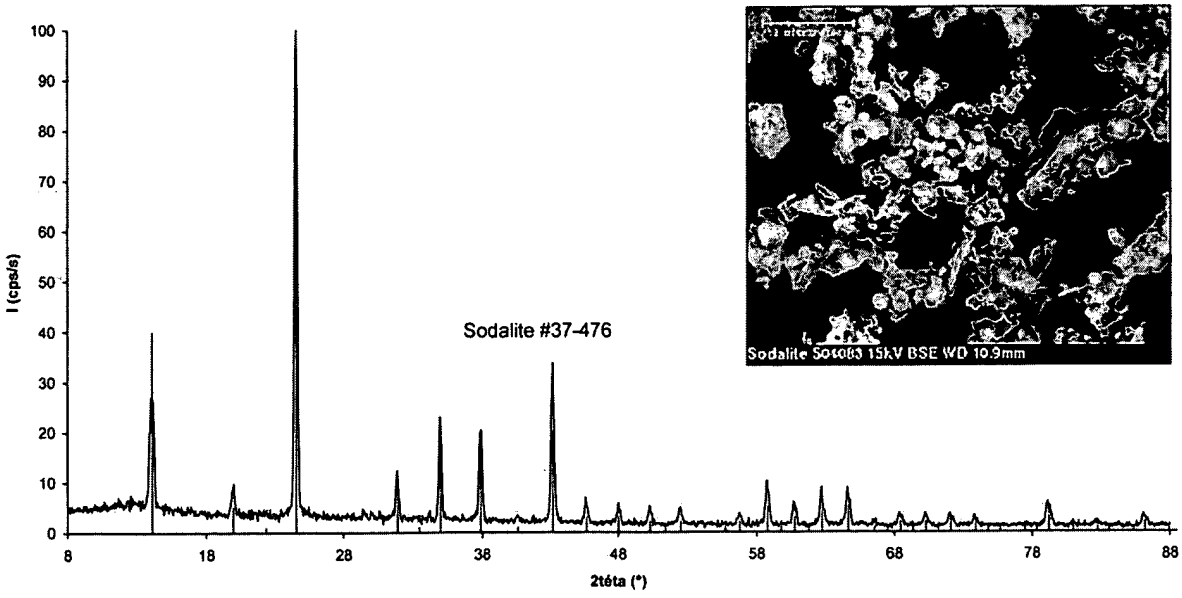

Fig. 9. XRD diagram and SEM image of sodalite powder ($Na_6Li_{1.2}K_{0.8}Al_6Si_6O_{24}Cl_2$) synthesized by heat treatment of a mixture nepheline and LiCl–KCl for 48 h at 700 °C.

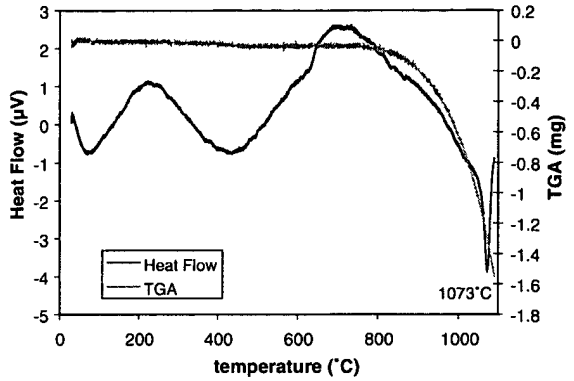

Fig. 10. DTA/TGA of sodalite powder after calcining for 48 h at 700 °C.

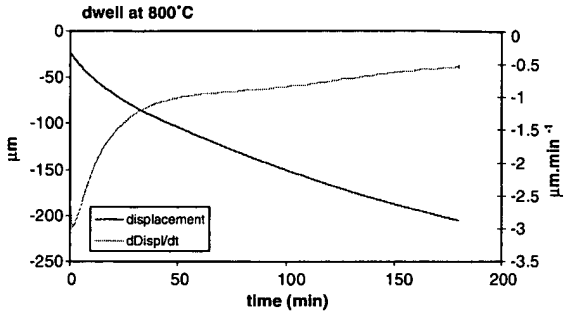

Fig. 11. Dilatometry measurement for 3 h at 800 °C of a sodalite pellet pressed at 100 MPa.

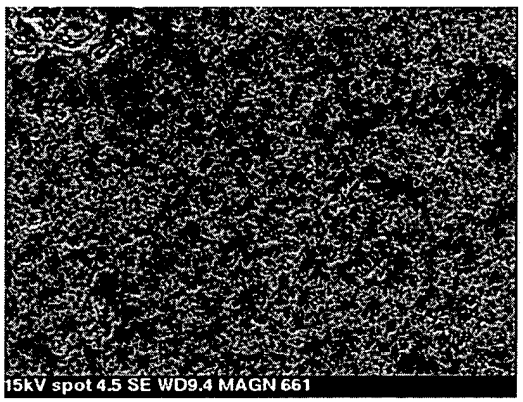

(a)

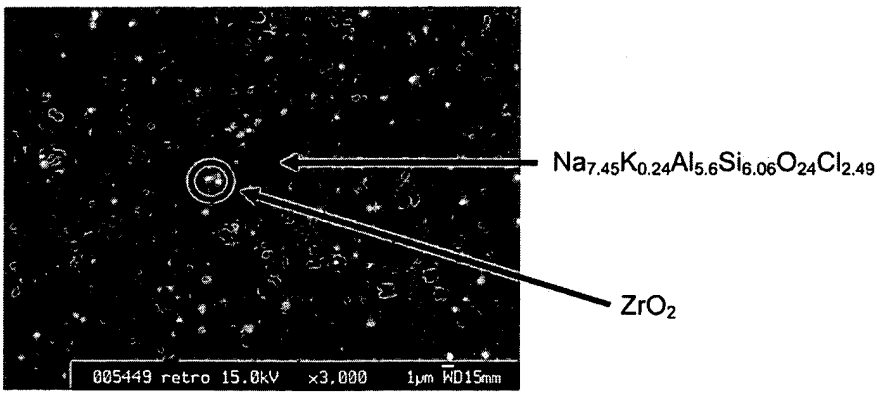

(b)

Fig. 12. SEM images of sintered sodalite pellets: (a) natural sintering for 15 h at 800 °C of a pellet pressed at 200 MPa ($d = 75\%d_{th}$). (b) Uniaxial pressure-assisted sintering for 5 h at 800 °C and 25 MPa ($d = 95\%d_{th}$).

indicated by the endothermic peak (Fig. 10). We therefore proceeded the sintering of sodalite at 800 °C. A dilatometry test was performed at this temperature for 3 h on a pellet pressed at 100 MPa (Fig. 11). Shrinkage was observed throughout the residence time at this temperature, but the shrinkage rate diminished over time. The rate variation curve versus time can be extrapolated to determine the moment at which the rate becomes zero, i.e. the time at which shrinkage ceases at this temperature: $5\frac{1}{2}$ h.

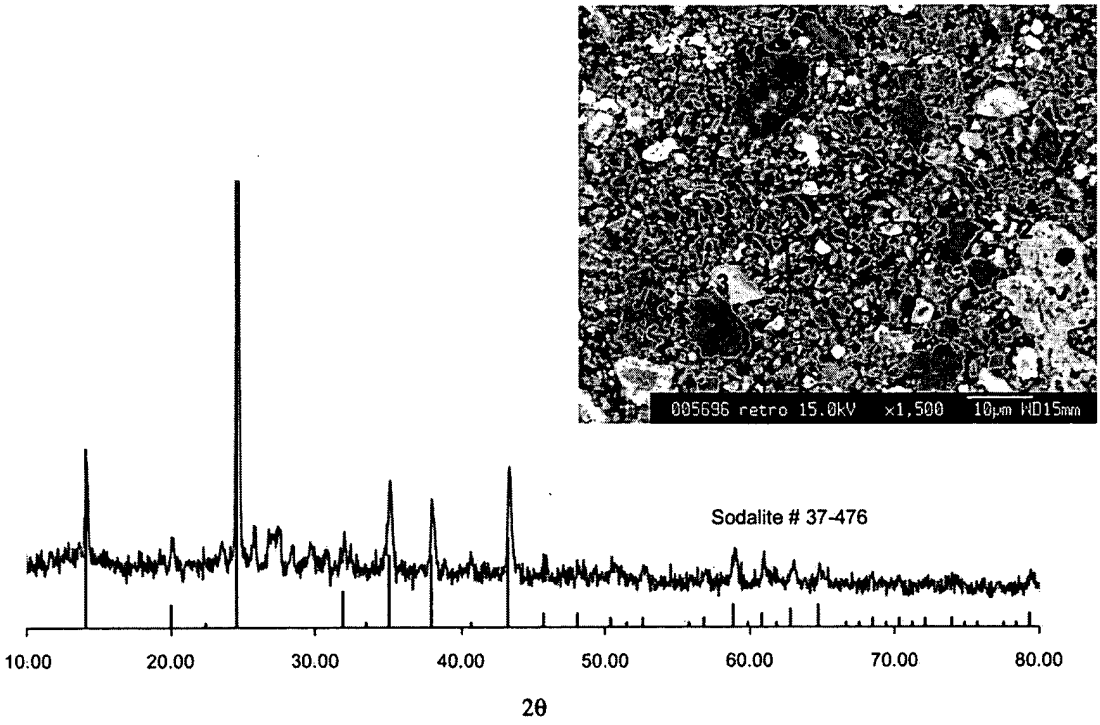

Fig. 13. XRD diagram and SEM image of sodalite powder synthesized by heat treatment of a mixture nepheline and lithium, potassium, barium, and strontium chlorides for 48 h at 700 °C.

Table 5
Wasteform quantities generated for 100 g of contaminated salt

Salt	Solvent (LiCl–KCl–εNaCl)			91 g
	FP chlorides			9 g
	Total			100 g
			Mass	Volume
LLW	Dechlorination/vitrification	AgCl	250 g	50 cm^3
		Or wadalite	500 g	170 cm^3
		Or calcium chlorosilicate[a]	250 g	~100 cm^3
		Or Cl recycling	_[b]	_[b]
	Direct immobilization	None	0 g	0 cm^3
HLW	Dechlorination/vitrification	Borosilicate glass at ~1.5 FP oxide wt%	500 g	185 cm^3
	Direct immobilization	Sodalite[c]	860 g	370 cm^3
		Or glass/sodalite composite	1100 g	450 cm^3

[a] +~30 g of alumina (7.5 cm^3).
[b] Non-quantified.
[c] Assuming rare earth elements and cesium enter the sodalite structure.

On this basis, sintering test was carried out. A pellet pressed at 200 MPa was then sintered for 15 h at 800 °C, reaching 75% of the calculated density as determined by geometrical measurements and scanning electron microscopic observation (Fig. 12(a)). In addition to the natural sintering test, an uniaxial pressure-assisted sintering test was carried out for 5 h at 800 °C and at 25 MPa. Although the specimen was fragmented along the compression axis on removal from the die, suggesting excessive pressure, the relative density of the fragments was 95% (Fig. 12(b)).

Then we evaluated the possibility of loading fission products in the sodalite structure. Sodalite was synthesized from nepheline and lithium, potassium, barium, and strontium chlorides under the same conditions. The resulting powder was characterized by XRD and appeared to consist mainly of sodalite. This was confirmed by microscopic examination (Fig. 13) of a poorly densified pellet showing three sodalite phases of variable composition.

3. Discussion

In order to compare the two management options of the contaminated salt (dechlorination–vitrification versus direct immobilization) waste quantities generated to process 100 g of contaminated salt were estimated and are reported in Table 5. These values are very high and suggest the necessity to increase the amount of FP in the salt prior to the treatment. Indeed, the current amount of FP in the salt is about 9 wt% [6]. The first option seems to produce less HLW than the second one. Moreover, if it was possible to confine alkaline earth metals in the sodalite structure, there is no proof that cesium (large radius nuclide) could be incorporated. Therefore, we have to consider the glass–sodalite composite option suggested by ANL [5], producing even more waste. Increasing the sodalite cage to make possible the containment of Cs in sodalite should be considered by substituting Al by Fe for example in further developments.

4. Conclusion

Two different routes can be taken to manage chlorinated salt streams contaminated by fission products from pyrochemical reprocessing of spent nuclear fuel. The salt can be converted to a vitrifiable mixture of oxides and hydroxides and the chlorine recovered in a form compatible with the immobilization in a suitable ceramic matrix, or recycled as a salt in the pyrochemical separation process; or a suitable containment matrix can be developed for chlorinated salt comprising mainly LiCl and KCl but contaminated by radioactive alkaline earth and rare earth elements. The feasibility of the first option was demonstrated by describing a chloride-to-oxyhydroxide conversion cycle and proposing solutions for chlorine immobilization in chlorosilicates such as wadalite ($Ca_6Al_5Si_2O_{16}Cl_3$) or calcium chlorosilicate ($Ca_3SiO_4Cl_2$).

Concerning the second option, phases capable of loading chlorides were reviewed and the initial synthesis tests of sodalite doped with alkalis and alkaline earths confirmed the potential of this phase for immobilizing chlorinated fission product waste.

This work constitutes a starting point to be further develop in the near future, particularly for the first option, separation of lithium and potassium chlorides from the other alkaline chlorides will be studied in order to reduce waste volumes and for the second option syntheses and characterization of oxochloride phases will have to be attempted.

References

[1] T. Nishimura, T. Koyama, M. Iizuka, H. Tanaka, Prog. Nucl. Energy 32 (3/4) (1998) 381.
[2] I.N. Taylor, M.L. Thompson, T.R. Johnson, Proceedings of the International Conference and Technology Exposition on Future Nuclear, Vol. 1, 1993, p. 690.
[3] S. Siwadamrongpong, M. Koide, K. Matusita, J. Non-Cryst. Solids 347 (2004) 114.
[4] M.K. Andrews, C.C. Saur, Conf-950811-9, WSRC-MS-95-0087, a document prepared for Mixed Waste Symposium at Baltimore from 08/07/95–08/11/95.
[5] M.A. Lewis, C. Pereira, United State Patent 5613240, 1997.
[6] C. Pereira, in: Proc. Ann. Meeting, Cincinnati, 1–3 May 1995, Ceram. Trans., p. 389.
[7] S.M. Frank, K.J. Bateman, T. DiSanto, S.G. Johnson, T.L. Moschetti, M.H. Noy, T.P. O'Holleran, MRS Fall 1997 Meeting 481 (1998) 351.
[8] C.W. Bale, P. Chartrand, S.A. Degterov, G. Eriksson, K. Hack, R. Ben Mahfoud, J. Melançon, A.D. Pelton, S. Petersen, Calphad 26 (2) (2002) 189.
[9] C. Sombret, J. Nucl. Mater. 82 (1) (1979) 163.
[10] T. Koyama, United States Patent 5340506, 1992.
[11] T. Koyama, C. Matsubara, T. Sawa, H. Tanaka, Central Research Institute of Electric Power Industry, 1998.
[12] J.C. Buhl, J. Solid State Chem. 91 (1991) 16.
[13] J.C. Buhl, J. Cryst. Growth 108 (1991) 143.
[14] A. Mere, D. Hyvonen, I. Heinmaa, T. Ruus, Proc. SPIE, The Int. Soc. Opt. Eng. 4318 (2001) 301.
[15] T. Hayashi, H. Shiga, M. Sadakat, T. Okubo, M. Yoshimura, J. Mater. Res. 13 (1998) 891.